



Figure 1. Temporal bones were processed according to the surface preparation method, and impregnated with RNAlater® (Ambion) to avoid the resolution of RNA. The membranous labyrinth was dissected. Arrows indicate pigmentation of stria vascularis.

a 5' fluorescent reporter dye and a 3' quencher dye were used. During the extension phase, Taq polymerase hydrolyzes the probe, thereby generating a

fluorescent signal. In our experiment, this signal was monitored using 7300 Real-Time PCR System® (Applied Biosystems).

Primer name	Sequences	Product size
COCH-F1	TGATGACATCGAGGAAGCAG	249
COCH-F2	ACAGGAAAAGCCTTGAAGCA	356
COCH-F3	GCCAGTGAACATCCCAAAT	461
COCH-F4	GCAGCGCCGATTTAATTTAC	555
COCH-F5	ACAAGCAGTGTCCACAGCAC	681
COCH-F6	GGCATCCAGTCTCAAATGCT	764
COCH-F7	TCCACAGGGGAGTAATCAGC	853
COCH-F8	GAGGCTTGGACATCAGGAAA	976
COCH-R	CAGGTCTTGCTGCACATCAT	

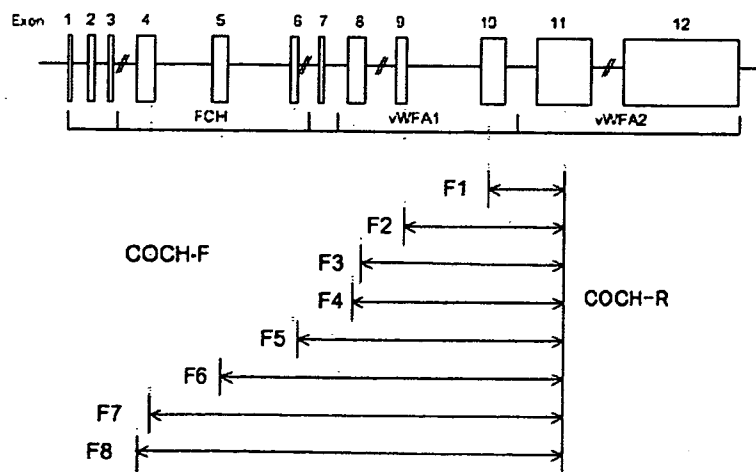


Figure 2. Primer sequences and amplified fragment size. Schematic drawing of the locus amplified by these primers in human *COCH* genomic structure. Exons are indicated by shaded boxes. The region of Limulus factor C homology (FCH) spans exon 4–6. The von Willebrand factor A-like domain, vWFA1, is contained in exon 8–10; vWFA2 is in exon 11 and 12. Each primer set is in coding region.

We measured levels of *GAPDH*, which is a well-known housekeeping gene. PCR primers and probes were provided by TaqMan<sup>®</sup> GAPDH Control Reagents kit (ABI). PCR was performed in a 20  $\mu$ l volume containing 10  $\mu$ l Premix Ex Taq<sup>®</sup> (Takara Bio, Otsu, Japan), 0.2  $\mu$ M of each specific primer, 0.1  $\mu$ l of the GAPDH probe, 0.4  $\mu$ l of Rox Reference Dye, and 1  $\mu$ l of cDNA from the RT reaction. After initial incubation at 95°C for 10 s, the reaction mixtures were subjected to 45 cycles of amplification using the following sequence: 95°C for 5 s and 60°C for 31 s. This was followed by a final extension step: 95°C for 15 s, 60°C for 1 min and 95°C for 15 s. TaqMan PCR<sup>®</sup> was performed twice for each sample.

To quantify mRNA for PCR levels, we recorded the average number of PCR cycles (Ct) required for each reaction's fluorescence to cross a threshold value of intensity, set to pass through the linear portion of the amplification curve. Frozen samples were defined as standards, and the difference in Ct between the formalin-fixed samples and the standards was used to calculate  $\Delta$ Ct. The quantity relative to the standard was obtained from  $2^{-\Delta$ Ct} [14]. The Student's *t* test was used for comparison between the two groups, and a probability value <0.05 was considered statistically significant.

## Results

### Total RNA yield

Average total RNA yield measured by ND-1000 Spectrophotometer<sup>®</sup> was  $0.89 \pm 0.40$   $\mu$ g of formalin-fixed samples and  $2.73 \pm 1.11$   $\mu$ g of frozen samples.

### Comparison of the length of RT-PCR products for frozen and formalin-fixed samples

The results of the *COCH* mRNA RT-PCR amplification are shown in Figure 3a and b, in comparison to the RT-PCR product migration in the gel with the migration of a 50 bp ladder marker (lane 1). Lanes 2–9 show the results of the RT-PCR amplification using *COCH* primers. Amplification to 976 bp was possible in all three frozen samples. On the other hand, among the three formalin-fixed samples, two could be amplified to only 249 bp and the other could not be amplified with these primers. By sequencing the amplification product, these bands were confirmed as targeted locus.

### Comparison of the quantity of real-time RT-PCR products between frozen and formalin-fixed specimens

The frozen samples were determined as standards, and the difference in Ct value between formalin-fixed samples and these standards was defined as

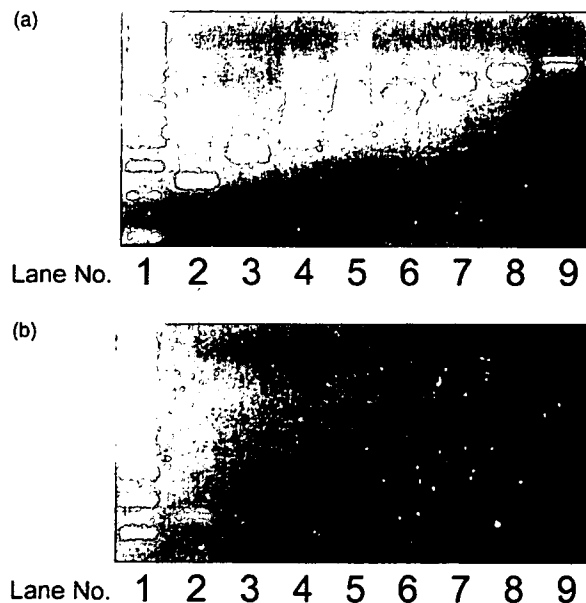


Figure 3. RT-PCR product migration in the gel with the migration of a 50 bp ladder marker (lane 1). Lanes 2–9 show the results of the RT-PCR amplification using *COCH* primers (a, frozen section; b, formalin-fixed sample). Amplification to 976 bp was possible in all three frozen samples; by contrast, two of the formalin-fixed samples could be amplified to only 249 bp and the other could not be amplified with these primers. Lane 2 shows a 249 bp fragment; lane 3, a 356 bp fragment; lane 4, 461 bp; lane 5, 555 bp; lane 6, 681 bp; lane 7, 764 bp; lane 853 bp; and lane 9, 976 bp.

Table I. Relative quantification using the comparative Ct method.

Conservation method	Average Ct	dCt (Ct - (Ct, frozen))	GADPH relative quantity to frozen sample
Frozen	27.37	0.00 ± 0.45	1.0 (0.7–1.4)
Formalin-fixation	33.65	-6.28 ± 0.56	0.012 (0.009–0.019)

The quantity of detectable GAPDH mRNA of frozen samples was defined as 1 while that of formalin-fixed samples was only 0.012.

dCt. As the efficiency of PCR is close to 1 according to Applied Biosystems guidelines, the value of  $2^{-dCt}$  shows the mRNA quantity of PCR level relative to that of the standards. The average relative quantity of the GAPDH RT-PCR product is shown in Table I. There was a significant difference between the two groups. Only about 1% of the quantity of PCR product of the frozen samples was obtained using formalin-fixed samples.

### Discussion

Analysis of inner ear function has progressed significantly from histological as well as molecular studies on experimental animals. In contrast, pathological study of the inner ear of humans with hearing loss is limited to cases in which brain autopsy is performed because it is impossible to access the inner ear during a patient's lifetime. Furthermore, the inner ear is present in hard bone tissue, and is highly differentiated anatomically and functionally. Therefore, it is difficult to study temporal bone molecular pathology by paraffin-embedded sections, nor can celloidin-embedded sections be relied upon [15].

To analyze real vital reactions at the molecular level, it is necessary to review manifestations of mRNA or protein. RT-PCR, in situ hybridization, Northern blot, or DNA microarrays for mRNA, and Western blot or immunostaining for protein are available for the analysis of vital reactions. However, these methods are usually difficult to apply to human inner ear specimens because these are usually formalin-fixed, celloidin-embedded specimens, which could easily degenerate and cause autolysis of fragile mRNA. Therefore, the human inner ear can be analyzed only for limited purposes. Lee et al. reported the first study of RT-PCR for archival temporal bones in 1997, in which they examined the manifestation of the  $\gamma$ -actin gene [16]. In this report, manifestation of  $\gamma$ -actin was detected in only 1 of 10 archival temporal bone specimens; the authors concluded that examination of the gene expression from an archival section was very limited because mRNA had been degraded by RNases. By contrast, Ohtani et al. reported that the  $\alpha$ -tubulin gene was identifiable to 79% by nested RT-PCR in archival temporal bones in 1999 [17]. They con-

cluded that the difference in their study from the former could be explained by the influence of primer design and RNA extraction methods. In formalin-fixed paraffin-embedded archival samples (liver tissue of mice), chemical modification such as methylol addition by formalin does not allow the direct application of extracted RNA to cDNA synthesis and RT-PCR [18].

In the present study, membranous labyrinths were dissected from three formalin-fixed and three frozen temporal bones and RNA was extracted from them. Then we compared the two samples based on how many base pairs of COCH mRNA were detectable. In addition, GAPDH mRNA was amplified by quantitative RT-PCR, and the quantities of RNA detectable by RT-PCR were compared. As a result, the COCH mRNA could be amplified to 976 bp in all the frozen sections, but among the formalin-fixed specimens, two could be amplified only to 249 bp while the other could not be amplified. In addition, the quantity of amplifiable GAPDH mRNA in the formalin-fixed specimens was only 1% of that of a frozen section. As a matter of course, both fragment lengths and quantities of RNA of formalin-fixed specimens are overwhelmingly smaller than those of frozen samples. Therefore, formalin-fixed temporal bone samples are not suitable for comprehensive molecular analysis, and conservation by freezing is desirable for introducing molecular pathological tools into human temporal bone pathology.

As for using autopsy specimens, Lin et al. reported RNA analysis of temporal bone soft tissues [10]. They collected temporal bones at immediate autopsies and showed manifestations and localizations of mRNA of mucin genes, such as MUC5B and MUC1, distributed in the submucosal gland of the eustachian tube and the middle ear, by Northern blot technique and in situ hybridization. They described how RNA degrades after death in a time-dependent manner, with the first obvious signs of degradation showing 6 h after death, and found mRNA was up to 1.4 kb in size at 6 h after death, indicating the preferability of an RNA analysis that uses molecular biological techniques within this time-frame.

However, in a regular clinical setting, it is not realistic to perform an autopsy within 6 h of death to obtain a temporal bone, not only from an ethical

perspective but also in terms of cooperation with a pathologist and the difficulty of processing specimens continuously. In our institution, removal of temporal bone specimens is included in the protocol of a conventional autopsy, and the average time from death to autopsy is 10 h. In this time, *COCH* mRNA could be amplified well up to 976 bp, which is the longest fragment expected by our primer planning. A continuous cryopreservation maneuver, which is routinely applied to preserve other organs, enables us to choose appropriate and effective analysis of precious cases. Therefore, our procedure is advantageous in that it can be performed in the protocol of a routine autopsy at any institution. Recently, Robertson et al. constructed a cDNA library from human fetuses at 16–22 weeks developmental age and reported that *COL1A2*, *COL2A2*, and *COL3A1*, which code types I, II, and III collagen, are intensely expressed by comparing expression levels with those of the brain by Northern blot technology [19]. They also reported that *COCH* emerged highly in the inner ear from the cDNA library, and these results led to the identification of *COCH* mutation causing DFNA9 [12,20,21]. Abe et al. extracted RNA from a cochlea obtained in an operation for acoustic neuroma or temporal bone tumor and reported that a strong manifestation of  $\mu$ -crystallin (*CRYM*) in the membranous labyrinth was shown by the cDNA microarray method [22]. Furthermore, they suggested that *CRYM* mutation causes nonsyndromic deafness by *CRYM*.

In contrast to studies using human fetuses or surgical specimens, we studied autopsy specimens and succeeded in extracting mRNA in comparatively good condition. Using our proposed technique, the human inner ear can be studied by both molecular and histopathologic methods. Therefore, when human temporal bone specimens with almost the same hearing levels on both sides are obtained, we recommend that one side be formalin-fixed and celloidin-embedded and examined morphologically, while the other side be frozen and analyzed for mRNA or other molecules. Comparison of morphological and molecular biological examinations may elucidate pathologies of sensory neural hearing loss at the cellular and molecular level.

## Conclusion

Well-preserved mRNA could be extracted from frozen human temporal bones removed at brain autopsy. The present study demonstrates that analysis of mRNA could be a clue in the study of molecular mechanisms of inner ear disorders using human temporal bones.

## Acknowledgements

We would like to thank to Mr Kenichi Koizumi for excellent technical support, and Prof. Yukiko Iino and Prof. Yoshihiko Murakami for technical advice. This study was supported by 21st Century COE Program Brain Integration and Its Disorder[s] and a Grant-in-Aid for Scientific Research (nos 14770888, 15790924, 14370539, 17390457, 16659462, 16790991, 17791163, 16012215, 18791194, 18791193) from the Ministry of Science, Education, Sports and Culture of Japan, and by Health and Labour Sciences Research Grants (H13-006; Research on Sensory and Communicative Disorders, and H14-21, H17-21 and no. 17242101; Research on Measures for Intractable Diseases) from the Ministry of Health, Labour and Welfare of Japan.

## References

- [1] Gibson F, Walsh J, Mburu P, Varela A, Brown KA, Antonio M, et al. A type VII myosin encoded by the mouse deafness gene shaker-1. *Nature* 1995;374:62–4.
- [2] Everett LA, Belyantseva IA, Noben-Trauth K, Cantos R, Chen A, Thakkar SI, et al. Targeted disruption of mouse *Pds* provides insight about the inner-ear defects encountered in Pendred syndrome. *Hum Mol Genet* 2001;10:153–61.
- [3] Schuknecht H. Pathology of the ear, 2nd edn. Philadelphia: Lea & Febiger; 1993.
- [4] Wackym PA, Simpson TA, Gantz BJ, Smith RJ. Polymerase chain reaction amplification of DNA from archival celloidin-embedded human temporal bone sections. *Laryngoscope* 1993;103:583–9.
- [5] Wacym PA, Popper P, Kerner MM, Grody WW. Varicella-zoster DNA in temporal bones of patients with Ramsay Hunt syndrome. *Lancet* 1993;342:1555.
- [6] Wackym PA. Molecular temporal bone pathology: II. Ramsay Hunt syndrome (*Herpes Zoster oticus*). *Laryngoscope* 1997;107:1165–75.
- [7] Seidman MD, Bai U, Khan MJ, Murphy MJ, Quirk WS, Castora FL, et al. Association of mitochondrial DNA deletions and cochlear pathology: a molecular biologic tool. *Laryngoscope* 1996;106:777–83.
- [8] Takahashi K, Merchant SN, Miyazawa T, Yamaguchi T, McKenna MJ, Kouda H, et al. Temporal bone histopathological and quantitative analysis of mitochondrial DNA in MELAS. *Laryngoscope* 2003;113:1362–8.
- [9] Kimura Y, Kouda H, Kobayashi D, Suzuki Y, Ishige I, Iino Y, et al. Detection of mitochondrial DNA from human inner ear using real-time polymerase chain reaction and laser microdissection. *Acta Otolaryngol (Stockh)* 2005;125:697–701.
- [10] Lin J, Kawano H, Paparella MM, Ho SB. Improved RNA analysis for immediate autopsy of temporal bone soft tissues. *Acta Otolaryngol (Stockh)* 1999;119:787–95.
- [11] Smith CA, Vernon JA. Handbook of auditory and vestibular research methods. Springfield, IL: Charles C Thomas; 1976. p. 5–51.
- [12] Robertson NG, Skvorak AB, Yin Y, Weremowicz S, Johnson KR, Kovatch KA, et al. Mapping and characterization of a novel cochlear gene in human and in mouse: a positional candidate gene for a deafness disorder, DFNA9. *Genomics* 1997;15:345–54.

- [13] Lehmann U, Glöckner S, Kleeberger W, von Wasielewski HF, Kreipe H. Detection of gene amplification in archival breast cancer specimens by laser assisted microdissection and quantitative real-time polymerase chain reaction. *Am J Pathol* 2000;156:1855–64.
- [14] Bloch G, Toma DP, Robinson GE. Behavioral rhythmicity, age, division of labor and period expression in the honey bee brain. *J Biol Rhythms* 2001;16:444–56.
- [15] Merchant SN, Burgess B, O'Malley J, Jones D, Adams JC. Polyester wax: a new embedding medium for the histopathologic study of human temporal bones. *Laryngoscope* 2006;116:245–9.
- [16] Lee KH, McKenna MJ, Sewell WF, Ung F. Ribonucleases may limit recovery of ribonucleic acids from archival human temporal bones. *Laryngoscope* 1997;107:1228–34.
- [17] Ohtani F, Furuta Y, Iino Y, Inuyama Y, Fukuda S. Amplification of RNA from archival human temporal bone sections. *Laryngoscope* 1999;109:617–20.
- [18] Masuda N, Ohnishi T, Kawamoto S, Monden M, Okubo K. Analysis of chemical modification of RNA from formalin-fixed samples and optimization of molecular biology applications for such samples. *Nucleic Acids Res* 1999;27:4436–43.
- [19] Robertson NG, Khetarpal U, Gutierrez-Espeleta GA, Bieber FR, Morton CC. Isolation of novel and known genes from a human fetal cochlear cDNA library using subtractive hybridization and differential screening. *Genomics* 1994;23:42–50.
- [20] Robertson NG, Lu L, Heller S, Merchant SN, Eavey RD, McKenna M, et al. Mutations in a novel cochlear gene cause DFNA9, a human nonsyndromic deafness with vestibular dysfunction. *Nat Genet* 1998;20:299–303.
- [21] Robertson NG, Cremers CW, Huygen PL, Ikezono T, Krastins B, Kremer H, et al. Cochlin immunostaining of inner ear pathologic deposits and proteomic analysis in DFNA9 deafness and vestibular dysfunction. *Hum Mol Genet* 2006;15:1071–85.
- [22] Abe S, Katagiri T, Saito-Hisaminato A, Usami S, Inoue Y, Tsunoda T, et al. Identification of CRYM as a candidate responsible for nonsyndromic deafness, through cDNA microarray analysis of human cochlear and vestibular tissues. *Am J Hum Genet* 2003;72:73–82.